

# Comparison of SNR and CNR for *in vivo* mouse brain imaging at 3 and 7 T using well matched scanner configurations

M. W. DiFrancesco<sup>a)</sup>

*Pediatric Neuroimaging Research Consortium, Imaging Research Center, Department of Radiology, Cincinnati Children's Hospital Medical Center, Cincinnati, Ohio 45229*

J. M. Rasmussen

*Imaging Research Center, Department of Radiology, Cincinnati Children's Hospital Medical Center, Cincinnati, Ohio 45229*

W. Yuan

*Pediatric Neuroimaging Research Consortium, Imaging Research Center, Department of Radiology, Cincinnati Children's Hospital Medical Center, Cincinnati, Ohio 45229*

R. Pratt, S. Dunn, and B. J. Dardzinski

*Imaging Research Center, Department of Radiology, Cincinnati Children's Hospital Medical Center, Cincinnati, Ohio 45229*

S. K. Holland

*Pediatric Neuroimaging Research Consortium, Imaging Research Center, Department of Radiology, Cincinnati Children's Hospital Medical Center, Cincinnati, Ohio 45229*

(Received 9 January 2008; revised 25 June 2008; accepted for publication 16 July 2008; published 8 August 2008)

Signal-to-noise ratio (SNR) and contrast-to-noise ratio (CNR) for magnetic resonance microimaging were measured using two nearly identical magnetic resonance imaging (MRI) scanners operating at field strengths of 3 and 7 T. Six mice were scanned using two imaging protocols commonly applied for *in vivo* imaging of small animal brain: RARE and FLASH. An accounting was made of the field dependence of relaxation times as well as a small number of hardware disparities between scanner systems. Standard methods for relaxometry were utilized to measure T1 and T2 for two white matter (WM) and two gray matter (GM) regions in the mouse brain. An average increase in T1 between 3 and 7 T of 28% was observed in the brain. T2 was found to decrease by 27% at 7 T in agreement with theoretical models. The SNR was found to be uniform throughout the mouse brain, increasing at higher field by a factor statistically indistinguishable from the ratio of Larmor frequencies when imaging with either method. The CNR between GM and WM structures was found to adhere to the expected field dependence for the RARE imaging sequence. Improvement in the CNR for the FLASH imaging sequence between 3 and 7 T was observed to be greater than the Larmor ratio, reflecting a greater susceptibility to partial volume effects at the lower SNR values at 3 T. Imaging at 7 T versus 3 T in small animals clearly provides advantages with respect to the CNR, even beyond the Larmor ratio, especially in lower SNR regimes. This careful multifaceted assessment of the benefits of higher static field is instructive for those newly embarking on small animal imaging. Currently the number of 7 T MRI scanners in use for research in human subjects is increasing at a rapid pace with approximately 30 systems deployed worldwide in 2008. The data presented in this article verify that if system performance and radio frequency uniformity is optimized at 7 T, it should be possible to realize the expected improvements in the CNR and SNR compared with MRI at 3 T. © 2008 American Association of Physicists in Medicine.

[DOI: [10.1118/1.2968092](https://doi.org/10.1118/1.2968092)]

Key words: contrast to noise ratio, signal to noise ratio, field strength dependence, image quality, mouse brain, relaxometry, 3 T MRI, 7 T MRI, radiofrequency coils

## I. INTRODUCTION

Since the introduction of *in vivo* magnetic resonance imaging (MRI),<sup>1</sup> there has been a trend toward the use of increasing static magnetic field strength ( $B_0$ ), motivated by improved performance at higher field strength. For some types of contrast, most notably blood oxygenation level dependent contrast (BOLD effect), that forms the basis of functional MRI studies, enhancement with field strength has been

demonstrated.<sup>2</sup> On theoretical grounds, an improvement in the signal-to-noise ratio (SNR) and the tissue contrast-to-noise ratio (CNR) is also expected in conventional imaging as a function of static field magnitude.<sup>3</sup> For human imaging, the field dependence, accounting for characteristics of the coil and sample, is expected to be linear.<sup>4</sup>

At field strengths exceeding 3 T, practical limitations can diminish improvement in image quality. T1 lengthens as the

field is increased creating a greater time burden on T2-weighted imaging.<sup>5-7</sup> Attainment of T1 spin echo contrast between white and gray matter of the brain is more challenging at higher B0 due to the requirement of a longer TR as well as the convergence of T1 values in these tissues.<sup>6,8</sup> The Larmor frequency of approximately 300 MHz at 7 T results in an radio frequency (RF) wavelength approaching the size of the human head which can result in interference patterns that cause spatially dependent RF field variations (B1) and inhomogeneous RF excitation in larger samples. In addition, artifacts arising from magnetic susceptibility gradients or chemical shift effects become more pronounced with an increase in static field.<sup>9,10</sup>

One study comparing 4 and 7 T verified a linear trend in SNR with field strength for human brain imaging using similar spin density-weighted sequence parameters and head coil configurations.<sup>11</sup> The SNR was found to agree favorably with the Larmor frequency ratio, averaged over the entire brain. Regional variation of the SNR was considerable, however, and dependent on the inhomogeneous distribution of the RF field. Using a Turbo SE protocol for microimaging in much smaller samples (rat brain), Beuf *et al.*<sup>12</sup> reported a failure to reach theoretical improvement in the SNR between 1.5 and 7 T. Notably, these investigators acknowledged that compensation had not been made for important differences in scanner RF chains and tissue relaxation parameters. The present study concentrates on high-resolution small animal conventional imaging using conventional protocols. Isolating the source of the SNR improvement between 3 and 7 T to the static field increase was facilitated by using well-matched MRI systems characterized well enough to compensate for remaining hardware differences impacting signal or noise. The small sample size and custom coil design assured uniform RF field contours. Identical imaging parameters were applied at both field strengths to minimize the complexity of comparison. Finally, T1 and T2 relaxation times were measured for mouse brain at both levels of B0 allowing compensation for relaxation effects on signal strength.

We attempt to concisely present in a single document all issues related to improvement in MRI performance with magnetic field strength and as such provide a useful reference document for scientists and investigators who are exploring the use of high field MRI. With current marketing trends and proliferation of 7 T MRI systems for human research applications, the results reported here may also be of importance to researchers and administrators seeking to justify the decision to invest in higher field MRI scanners for human investigations. It is evident from our results in mice that a 7 T MRI system, with optimally designed RF systems to achieve B1 homogeneity in the sample, can indeed deliver near-theoretical improvements SNR and CNR over a comparable 3 T scanner.

## II. THEORY

The SNR expected in a magnetic resonance (MR) measurement with a well matched and tuned coil is routinely written as<sup>3,13</sup>

$$\text{SNR} = \frac{\omega M_0 \hat{B}_1 \Delta V}{\sqrt{4kT(r_c + r_s) \Delta \nu}}, \quad (1)$$

where  $\omega$  is the resonant frequency,  $M_0$  ( $\propto \omega$ ) is the magnetization due to the static field,  $\hat{B}_1$  refers to the magnetic field induced at the position of a sample volume element,  $\Delta V$ , by unit current flowing in the coil,  $k$  is the Boltzmann's constant,  $T$  is the sample temperature, and  $\Delta \nu$  is the detection bandwidth. Energy dissipation in the coil and the sample is expressed by an effective resistance,  $r_c$  and  $r_s$ , respectively. Sample dissipation ( $\propto \omega^2$ ), a function of conductivity, is also strongly dependent on sample size. The effective resistance of a conducting spherical sample, for instance, theoretically varies by the radius to the fifth power.<sup>3</sup> When imaging the human brain, sample dissipation usually exceeds the contribution from the coil. According to Eq. (1), the SNR is expected to depend linearly on field strength when sample resistance dominates. Coil dissipation may be significant, however, when imaging small animals. The frequency dependence of the coil's effective resistance, nominally arising from the skin effect ( $\propto \omega^{1/2}$ ), often needs to account for details of coil geometry.

The quality factor of a RF coil,  $Q = \omega L / (r_c + r_s)$ , where  $L$  is the coil inductance, is often used to characterize dissipation in practice. For convenience we can express the SNR in Eq. (1) in terms of  $Q$ , which is easy to measure, as follows:

$$\text{SNR} = \frac{\sqrt{\omega Q} M_0 \hat{B}_1 \Delta V}{\sqrt{4kTL \Delta \nu}}. \quad (2)$$

The CNR between two regions of an image, designated region 1 and region 2, is defined as the difference in SNR between those regions

$$\text{CNR}_{12} = \text{SNR}_1 - \text{SNR}_2. \quad (3)$$

The CNR serves as a measure of how well features can be distinguished in an image and, as a result of Eq. (3), should have the same frequency dependence as the SNR.

## III. MATERIALS AND METHODS

### III.A. MR scanners

Two Bruker scanners (Bruker BioSpin MRI, Ettlingen, Germany) were employed for this study; a BioSpec 30/60 and a BioSpec 70/30 with attributes listed in Table I. The scanners were equipped with identically designed 20 cm gradient coils driven by the same model of Copley gradient amplifiers and operated under the same software.

Maximum current limits were set differently for the two systems as indicated in Table I. RF electronics on both scanners were at current revisions of the Bruker AVANCE™ platform. The RF receive channel noise figure was measured for each system and considered for noise analysis. Both scanners were situated in shielded rooms.

TABLE I. Attributes of scanners used in this study.

Attribute	Scanner	
	Biospec 30/60	Biospec 70/30
Field strength (Larmor frequency)	<b>2.94 T (125.3 MHz)</b>	<b>7.05 T (300.3 MHz)</b>
Gradient configuration (20 cm diam)	B-GA 20 S2	B-GA 20 S2
Gradient amplifier	Copley 265	Copley 265
Maximum gradient strength	42533 Hz/cm	81999 Hz/cm
Software	ParaVision v.3.0.2	ParaVision v.3.0.2
Shim system	BS60 (60 cm diam)	BS30 (30 cm diam)
Preamp	Bruker XBB module	Bruker 1H module
RF pulse amplifier	American Microwave Technologies 3435	Bruker BLAH-1000
RF transmit/receive coil	25 mm single turn solenoid	25 mm single turn solenoid
RF receive channel noise figure <sup>a</sup>	2.6 dB	1.6 dB

<sup>a</sup>Averaged over a range of typical gains.

### III.B. RF coils

A pair of identical, single-turn-solenoid RF coils were constructed for this comparison, each tuned and matched for its respective scanner environment. This design was chosen for its high  $Q$  and excellent RF field homogeneity. The ease of construction of these coils was also a benefit as they were custom-built to measure 25 mm in diameter and 30 mm in length to closely accommodate a mouse head (Fig. 1). These circumstances evaded sensitivity to sample placement as might be expected in a more conventional surface coil configuration. The cylindrical solenoid was constructed of 50  $\mu\text{m}$  thick copper sheet formed in two halves leaving two longitudinal gaps along which tuning capacitance was evenly distributed. A matching circuit was inductively coupled to the main coil by a coaxial wire loop of the same diameter. The B1 field distribution was assessed using a double-angle MRI method<sup>14</sup> with a homogeneous gadolinium-doped sample. The unloaded/loaded  $Q$  of the coils was measured via network analyzer using a vial of normal saline solution as a load for convenience. The loading of the saline sample was found to closely mimic that of a mouse.

### III.C. Mice

Six healthy FVB/N wild type female mice were used for this study. Ages ranged from 3 to 4 months with weights of 17–23 g. During scanning, the mice were anesthetized using



Fig. 1. Single turn solenoid coils. 7 and 3 T coil pictured left and right, respectively.

2% Isoflurane in air, bitebar stabilized, and monitored to maintain an approximate respiration rate of 50 cycles/min. The mouse bed was maintained at 35–40 °C using warm water flow. IACUC approval for the study protocol (No. 4A04034) was obtained after review at Cincinnati Children's Research Foundation.

### III.D. Relaxometry

T1 and T2 relaxation time maps were generated within a single coronal slice of each mouse brain at Bregma  $-1.5$  mm, which includes a variety of recognizable white matter (WM) and gray matter (GM) structures; corpus callosum, hippocampus, inner capsule, and outer cortex. T1 and T2 measures were used to establish the dependence of relaxation on field strength between 3 and 7 T, to guide parameter choices for imaging, and to normalize signal strength for relaxation times. Single slice acquisition avoided contamination from neighboring slices.

T1 at 7 T was measured by an inversion recovery RARE method with TR/TE=13 000/8.2 ms, field of view (FOV)=2.56  $\times$  2.56 cm, matrix size=172  $\times$  172 voxels, slice thickness=0.4 mm, number of averages (NA)=1, and rare factor=4. At 3 T, the same protocol was used except TE =9 ms and slice thickness=1 mm. Nine images were generated with inversion times of 50, 80, 125, 175, 250, 500, 1000, 2000, 4000, and 8000 ms. For each pixel, intensity was plotted against inversion time and fitted by least squares to a three parameter exponential recovery function to determine T1.

T2 at 7 T was measured via a multiple echo spin-echo (SE) method with TR/TE=5000/10 ms, 64 echoes, FOV=1.92  $\times$  1.92 cm, matrix size=128  $\times$  128 voxels, and slice thickness=1 mm. The same protocol was used at 3 T, except the FOV was slightly larger at 2.2  $\times$  1.96 cm. It is well known that multiple echo sequences of this kind can suffer marked signal modulation due to imperfect refocusing pulses and static field inhomogeneity.<sup>15–17</sup> Including a combination of spoiler gradients in the slice direction, refocused phase encoding, and dephasing gradients in the read direction effectively eliminated image artifacts.<sup>18</sup> The remaining

signal modulation due to stimulated echoes was most severe for the first few echoes.<sup>18,19</sup> Consequently, data from the first three echo times were eliminated before image intensity was plotted against echo time for each pixel. The resulting signal time dependence was well described by a three-parameter single exponential decay function to which a least squares fit was made to determine T2.

### III.E. Imaging

For SNR comparisons, identical imaging protocols were executed for each mouse at both field strengths including a T2-weighted SE method and a  $\rho/T1$ -weighted ( $\rho$ =spin density) gradient-echo (GE) method. The protocols were deliberately chosen as examples of those in common use today for small animal imaging. Instead of optimizing imaging parameters for each field strength, identical parameter sets were employed in both scanners to minimize disparate effects of diffusion and motion that would otherwise arise through gradient strength and timing differences.

The SE method used a two-dimensional (2D) RARE protocol in a single coronal slice at Bregma  $-1.5$  mm with a slice thickness=0.5 mm, TR=3000 ms with flipback, rare factor=4, effective TE=40 ms, NA=4, BW=50 kHz, FOV =  $1.92 \times 1.92$  cm, and a matrix size of  $128 \times 128$ , resulting in a scan time of 6 min. 24 s.

A 2D FLASH protocol was employed for the GE method. Images were obtained at 3 and 7 T at the same coronal slice with TR/TE=150/6.7 ms, flip angle=40°, NA=4, BW =50 kHz, FOV= $1.92 \times 1.92$  cm, and a matrix size of  $128 \times 128$ . The scan time was 1 min. 17 s.

Imaging was prepared via automated routines incorporated in the Bruker PVM software. After brain localization at isocenter, global shimming, restricted to linear order terms, was completed. Excitation pulse power calibration was applied in an axial plane through isocenter.

### III.F. SNR and CNR calculations

The RARE 7 T image in the upper left panel of Fig. 3 shows representative regions of interest (ROIs) in four anatomic regions selected for this study, plus a ROI in artifact-free background to sample noise. The anatomic ROIs include two GM structures (cortex and hippocampus) and two WM structures (corpus callosum and internal capsule). RARE and FLASH images of each mouse were acquired during the same session in each scanner, maintaining their alignment. Since the RARE images exhibited superior contrast, they were used for drawing the ROIs. Alignment allowed the copying of ROIs from each RARE image to the corresponding FLASH image of the same session. This was not possible to do between different mice and field strengths, however, efforts were made to minimize the variation in ROIs drawn between sessions.

The average signal was estimated in each of the four anatomic ROIs for each mouse. The average signal in the corner ROI (labeled 5 in Fig. 2) provided a measure of  $\sim 1.25\sigma$ , where  $\sigma$  represents the image noise standard deviation described by a Raleigh distribution. Noise,  $\sigma$ , measured in each

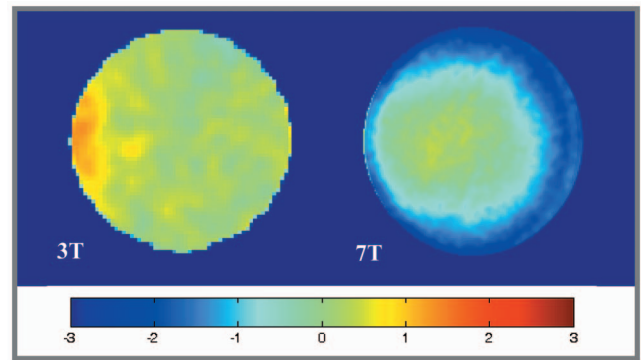


FIG. 2. B1 field profiles for the single turn solenoid RF coils at 3 (left) and 7 T. The profile is shown for a cross section near the center of the coil. Percent deviation of the field strength from the central value is indicated by color according to the colorbar.

scanner was further adjusted by a factor to compensate for differences in contribution from the RF receive chain derived from the noise figure (see Table I). An accounting of differences in receiver gain between scans was done for all signal measurements. The signal at 7 T was further adjusted relative to the 3 T signal to remove the influence of disparities in relaxation times. RARE signals were normalized for T2 differences according to the factor  $e^{-TE/T2}$ . The increase in T1 at 7 T was compensated in FLASH images by  $(1 - E)/[1 - E \cos(\alpha)]$ , where  $E = e^{-TR/T1}$  and  $\alpha$  is the flip angle. The ratio of the resulting average signal in each ROI to the compensated noise provided the measure of the SNR for this study. The SNR, defined this way, was calculated for each mouse, at both field strengths, using both RARE and FLASH methods of imaging. In addition, the ratio of the SNR at 7 T versus 3 T was determined for each individual mouse and averaged. This average SNR ratio was compared to the theoretically expected value of 2.40, the ratio of Larmor frequencies.

Treatment of the CNR was condensed by considering broadly the contrast between WM and GM. The SNR values for GM and WM were calculated for each mouse by averaging across the pair of ROIs corresponding to the respective tissue type. The CNR was then calculated for each mouse according to Eq. (3) and averaged across mice for each imaging method and field strength. Finally, the CNR ratio between 7 and 3 T was averaged across mice for each imaging method and compared to the Larmor frequency ratio.

## IV. RESULTS

### IV.A. RF coil characteristics

Inhomogeneity of the B1 field distribution was found to be modest, even at 7 T, with less than 3% variation across the region to be imaged in this experiment. B1 maps are shown in Fig. 2 for a centrally placed slice through the coil close to the position of the slice used for mouse imaging. This small sample/coil configuration, therefore, allows a uniform comparison of the SNR across images taken near this position.



TABLE II. *In vivo* relaxometry outcomes for four anatomic regions of mouse brain at 3 and 7 T.

Anatomic region	T1 (ms)		T2 (ms)	
	3 T	7 T	3 T	7 T
Corpus callosum	1108 ± 9	1405 ± 22	66.7 ± 0.7	52.5 ± 0.4
Internal capsule	913 ± 16	1239 ± 15	62.7 ± 1.1	49.3 ± 0.8
Hippocampus	1310 ± 15	1564 ± 8	73.1 ± 1.4	58.9 ± 1.2
Cortex	1246 ± 28	1612 ± 26	68.6 ± 0.9	52.7 ± 0.4

The unloaded/loaded  $Q$  of the coils was measured as 387/276 at 3 T and 160/98 at 7 T. Such a modest reduction in  $Q$  due to loading is consistent with coil-dominated resistance as one might expect for the small sample size. Even unloaded, the change in  $Q$  after increasing frequency is consistent with a  $1/\omega$  dependence, implying an  $\omega^2$  dependence of coil resistance. This behavior may be explained by the greater restriction of current density to the outer edges of the solenoid as well as along the surface of the copper sheet with increased frequency. According to Eq. (2), a linear dependence of the SNR with frequency is expected when using this coil design for small animal imaging.

#### IV.B. Relaxometry

Relaxation times for each field strength, averaged over all mice, for the four brain regions selected for this work are listed in Table II. The uncertainty indicated is the standard error of the mean across the six mice. As expected, WM tended to have shorter T1 and T2 than GM at a given field strength. On average across the mouse brain, going from 3 to 7 T increased T1 by about 28% and decreased T2 by 27%.

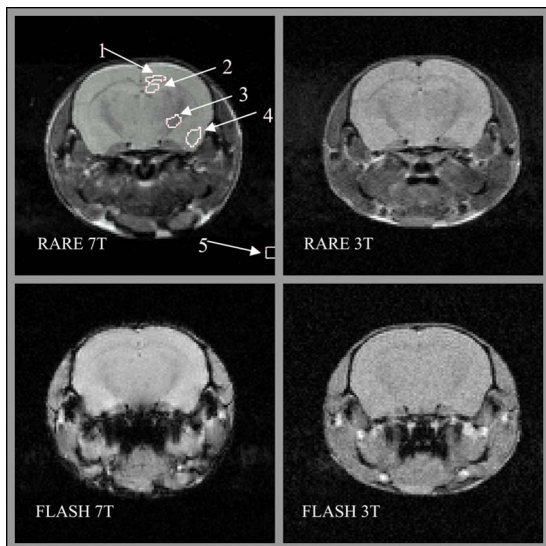


FIG. 3. Characteristic images using FLASH and RARE methods at 3 and 7 T as indicated. The RARE 7 T image includes typical regions of interest drawn for this study labeled with numbers. Two WM regions are identified: (1) Corpus callosum and (3) internal capsule. GM regions include: (2) Hippocampus and (4) cortex. Image noise is measured in (5) an artifact free background region.

TABLE III. Comparing the mean SNR at 7 and 3 T for various anatomic regions using the RARE method. The  $p$  value is for the difference between the measured mean SNR ratio and the value 2.40, the ratio of Larmor frequencies.

Anatomic region	Mean SNR at 7 T	Mean SNR at 3 T	Mean SNR ratio 7 T vs 3 T
Corpus callosum	98.7 ± 8.3	40.6 ± 1.8	2.46 ± 0.24 ( $p=0.81$ )
Internal capsule	89.9 ± 7.7	37.3 ± 1.6	2.44 ± 0.24 ( $p=0.84$ )
Hippocampus	105.0 ± 8.9	45.2 ± 1.9	2.35 ± 0.23 ( $p=0.87$ )
Cortex	110.0 ± 9.3	44.8 ± 1.8	2.48 ± 0.24 ( $p=0.75$ )

#### IV.C. Imaging, SNR and CNR

Figure 3 shows a side-by-side comparison of representative images of mouse brain acquired for this study. Tables III and IV summarize the outcomes for the RARE and the FLASH imaging protocol, respectively, by listing the mean SNR across the six mice for each anatomic region. These results are provided at 3 and 7 T. Stated uncertainties are the propagated error accounting for the standard error of the mean of the SNR measurements, as well as the error in the noise figure and relaxation factor corrections. While the improvement of the mean SNR going from 3 to 7 T was found to be equal to the Larmor ratio for all anatomic regions for the RARE imaging method, it was consistently higher among all anatomic regions for the FLASH imaging method. Deviation from the Larmor ratio was not found to be statistically significant, however, for any of the anatomical regions for either imaging method.

The mean SNR across mice for GM and WM tissues is listed in Table V according to imaging method and field strength. The mean CNR between GM and WM across mice is also listed at 3 and 7 T for both imaging methods. The far right column of Table V includes the mean ratio of the CNR values at 7 and 3 T for each imaging method accompanied by the  $p$  value for the difference from the Larmor ratio. The RARE data result in a CNR ratio that is in close agreement with the theoretical value. The mean CNR ratio for FLASH imaging, however, measured considerably greater than the expected value.

#### V. DISCUSSION AND CONCLUSIONS

Relaxometry outcomes included a 28% increase in T1 at 7 T that is in close agreement with the power law depen-

TABLE IV. Comparing the mean SNR at 7 and 3 T for various anatomic regions using the FLASH method. The  $p$  value is for the difference between the measured mean SNR ratio and the value 2.40, the ratio of Larmor frequencies.

Anatomic region	Mean SNR at 7 T	Mean SNR at 3 T	Mean SNR ratio 7 T vs 3 T
Corpus callosum	71.7 ± 6.0	28.2 ± 0.8	2.54 ± 0.21 ( $p=0.52$ )
Internal capsule	70.0 ± 5.9	26.9 ± 0.7	2.60 ± 0.22 ( $p=0.39$ )
Hippocampus	72.2 ± 6.1	29.3 ± 0.8	2.46 ± 0.21 ( $p=0.77$ )
Cortex	77.5 ± 6.5	28.8 ± 0.8	2.69 ± 0.23 ( $p=0.25$ )

TABLE V. Comparing the mean SNR of GM and WM, at 3 and 7 T, using each of the imaging methods. The mean CNR between GM and WM is also shown.

Imaging method	Field strength	Mean SNR GM	Mean SNR WM	Mean CNR GM-WM	Mean CNR ratio
<b>RARE</b>	7 T	107.5 ± 4.7	94.3 ± 4.0	14.6 ± 1.8	2.42 ± 0.28 ( $p=0.93$ )
	3 T	45.0 ± 1.8	38.9 ± 1.7	6.1 ± 0.6	
<b>FLASH</b>	7 T	74.8 ± 3.0	70.9 ± 2.7	5.8 ± 0.6	3.86 ± 0.45 ( $p=0.01$ )
	3 T	29.0 ± 0.8	27.5 ± 0.7	1.5 ± 0.1	

dence reported by Bottomley *et al.*<sup>20</sup> Though not theoretically predicted to vary with resonant frequency up to 100 MHz,<sup>21</sup> T2 is known to decrease substantially at higher frequencies principally due to chemical exchange between bound and bulk water in tissue.<sup>22</sup> A decrease of T2 between 1.5 and 4 T has been reported elsewhere in human brain.<sup>23</sup> The 27% decrease in T2 in a mouse brain reported here between 125 and 300 MHz substantiates this trend. T1 and T2 measurements at 7 T in a mouse brain have been published by other investigators.<sup>24</sup> Their work, using different relaxometry protocols, produced a T1 that is slightly longer and a T2 that is somewhat shorter than those reported here for corresponding anatomic regions.

Improvement of small animal *in vivo* MR microimage quality resulting from an increase in static magnetic field strength from 3 to 7 T has been assessed in this study. Starting with similarly configured scanner systems, corrections were made for all remaining differences in hardware that impact signal or noise. The signal was normalized with respect to receiver gain and disparities of T1 and T2 relaxation times while noise measurements were compensated for noise figure differences. After isolation of system differences to field strength to this extent, the *in vivo* mouse brain image SNR was found to increase by a factor equal to the ratio of Larmor frequencies, as expected for the sample/coil configuration used. Since the SNR ratio across brain regions was found to be homogeneous, one can expect the CNR between regions to have the same dependence on field strength. Indeed, the same improvement in the CNR was measured between 3 and 7 T for spin-echo RARE imaging. In contrast, improvement in the CNR between field strengths exceeded the Larmor ratio for FLASH imaging. The SNR for the 3 T FLASH, though having expected values compared to the 7 T FLASH, is low enough to be sensitive to mixing of WM and GM signal due to partial volume effects and to imperfect delineation of small anatomic structures by the ROIs drawn on the images.

Besides the inadequate image quality achieved at 3 T, the FLASH protocol comparison at the two field strengths suffered from additional shortcomings. Though an attempt was made to employ the shortest TE possible that was compatible with both imaging systems, limitations of the 3 T system restricted TE to 6.7 ms. This value of TE leaves the FLASH imaging method sensitive to differences in T2\* in the regime of B0 considered here. Measurement of T2\* was not carried out on the mice used in this work, but published human and

small animal studies<sup>5,6,25</sup> allow reasonable estimates of T2\* in the brain of about 40 and 25 ms at 3 and 7 T, respectively. Abiding by such estimates, the normalization of signal strength according to an exponential decay at the rate of TE/T2\* would result in a further increase of the 7 T/3 T SNR ratio reported here of about 10%.

FLASH imaging is also sensitive to disparities in B0 uniformity. This comparison of the SNR and CNR in a mouse brain at 3 and 7 T employed only first order shimming of the samples so that the degree of correction for field heterogeneity of the two magnets would be more consistent for the comparison. Higher order shimming could improve the B0 uniformity and possibly improve the SNR and CNR at both field strengths. One could argue that magnetic susceptibility gradients inherent in a mouse brain would produce field dependent perturbations in B0 homogeneity, thereby producing more severe degradation of the SNR at 7 T than at 3 T. Consequently, high order shimming might produce further improvements at 7 T relative to 3 T. Our 7 T Biospec 70/30 system was equipped with high power second order shims and shim power supplies that allow for shim fields up to 100 Hz/cm<sup>2</sup>. These shims are built into the B-GA 20 S2 gradient set for the 7 T system. However, the shims on the 3 T system are built into a separate shim subsystem in the 60 cm 3 T magnet assembly. Consequently, correction for second order and higher order field inhomogeneities is not comparable for the two systems. We chose to eliminate this variable from our comparison. Given that the ratio of the SNR between 7 and 3 T closely approximates the predicted value for FLASH imaging, it does not appear that the lack of higher order shimming caused any disadvantage for the 7 T images. However, a further increase in the 7 T/3 T SNR ratio, normalized according to linewidth, cannot be ruled out.

The sensitivity of the induction-coupled coils used for this comparison is susceptible to vibration, particularly from applying gradients, via the resulting fluctuations in mutual inductance. This effect was not specifically measured for this study, but it is reasonable to assume that the relative amount of signal change was the same for both scanners, thereby not affecting the comparison.

At field strengths beyond 7 T it is likely that B1 uniformity may suffer with conventional single phase or quadrature phase RF coils. In this case, predicted improvements in the SNR may not be realized unless phased array coils are employed, as is now the case with high field human systems.<sup>11</sup>

The results of this study verify that increases in magnetic field strength yield predicted increases in the SNR and therefore, resolution in MR images of small animals. If the SNR is large enough at lower field strengths, the CNR will improve to the same degree. However, more challenging circumstances resulting in poor SNR or resolution at lower field will find the CNR improving even more markedly as field strength is increased.

## ACKNOWLEDGMENTS

Work supported in part by NIBIB: T32-EBO1656 (PI: W. Ball) and P30 AR47363-01. The authors also thank Bruker BioSpin MRI GmbH, Ettlingen, Germany.

- <sup>a)</sup> Author to whom correspondence should be addressed. Present address: Cincinnati Children's Hospital Medical Center, 3333 Burnet Ave., ML 5033, Cincinnati, OH 45229. Telephone: (513) 636-0436. Fax: (513) 636-3754. Electronic mail: mark.difrancesco@cchmc.org
- <sup>1</sup>P. C. Lauterbur, "Image formation by induced local interactions: Examples employing nuclear magnetic resonance," *Nature (London)* **242**, 190–191 (1973).
- <sup>2</sup>G. Kruger, A. Kastrup, and G. H. Glover, "Neuroimaging at 1.5 T and 3.0 T: Comparison of oxygenation-sensitive magnetic resonance imaging," *Magn. Reson. Med.* **45**, 595–604 (2001).
- <sup>3</sup>C.-N. Chen and D. I. Hoult, *Biomedical Magnetic Resonance Technology* (Adam Hilger, New York, 1989).
- <sup>4</sup>C. N. Chen, V. J. Sank, S. M. Cohen, and D. I. Hoult, "The field dependence of NMR imaging. I. Laboratory assessment of signal-to-noise ratio and power deposition," *Magn. Reson. Med.* **3**, 722–729 (1986).
- <sup>5</sup>P. Jezzard, S. Duewell, and R. S. Balaban, "MR relaxation times in human brain: Measurement at 4 T," *Radiology* **199**, 773–779 (1996).
- <sup>6</sup>D. G. Norris, "High field human imaging," *J. Magn. Reson. Imaging* **18**, 519–529 (2003).
- <sup>7</sup>S. H. Koenig and R. D. Brown III, "Determinants of proton relaxation rates in tissue," *Magn. Reson. Med.* **1**, 437–449 (1984).
- <sup>8</sup>H. W. Fischer, P. A. Rinck, Y. Van Haverbeke, and R. N. Muller, "Nuclear relaxation of human brain gray and white matter: Analysis of field dependence and implications for MRI," *Magn. Reson. Med.* **16**, 317–334 (1990).
- <sup>9</sup>D. A. Yablonskiy and E. M. Haacke, "Theory of NMR signal behavior in magnetically inhomogeneous tissues: The static dephasing regime," *Magn. Reson. Med.* **32**, 749–763 (1994).
- <sup>10</sup>F. Schick, "Whole-body MRI at high field: Technical limits and clinical potential," *Eur. Radiol.* **15**, 946–959 (2005).
- <sup>11</sup>J. T. Vaughan, M. Garwood, C. M. Collins, W. Liu, L. DelaBarre, G. Adriany, P. Andersen, H. Merkle, R. Goebel, M. B. Smith, and K. Ugurbil, "7 T vs. 4 T: RF power, homogeneity, and signal-to-noise comparison in head images," *Magn. Reson. Med.* **46**, 24–30 (2001).
- <sup>12</sup>O. Beuf, F. Jaillon, and H. Saint-Jalmes, "Small-animal MRI: Signal-to-noise ratio comparison at 7 and 1.5 T with multiple-animal acquisition strategies," *MAGMA (N.Y.)* **19**, 202–208 (2006).
- <sup>13</sup>D. I. Hoult and B. Tomanek, "Use of mutually inductive coupling in probe design," *Concepts Magn. Reson.* **15**, 262–285 (2002).
- <sup>14</sup>R. Stollberger and P. Wach, "Imaging of the active B1 field *in vivo*," *Magn. Reson. Med.* **35**, 246–251 (1996).
- <sup>15</sup>A. P. Crawley and R. M. Henkelman, "Errors in T2 estimation using multislice multiple-echo imaging," *Magn. Reson. Med.* **4**, 34–47 (1987).
- <sup>16</sup>S. Majumdar, S. C. Orphanoudakis, A. Gmitro, M. O'Donnell, and J. C. Gore, "Errors in the measurements of T2 using multiple-echo MRI techniques. II. Effects of static field inhomogeneity," *Magn. Reson. Med.* **3**, 562–574 (1986).
- <sup>17</sup>S. Majumdar, S. C. Orphanoudakis, A. Gmitro, M. O'Donnell, and J. C. Gore, "Errors in the measurements of T2 using multiple-echo MRI techniques. I. Effects of radiofrequency pulse imperfections," *Magn. Reson. Med.* **3**, 397–417 (1986).
- <sup>18</sup>J. P. Wansapura, S. K. Holland, R. S. Dunn, and W. S. Ball, Jr., "NMR relaxation times in the human brain at 3.0 tesla," *J. Magn. Reson. Imaging* **9**, 531–538 (1999).
- <sup>19</sup>G. J. Stanisz, E. E. Odobina, J. Pun, M. Escaravage, S. J. Graham, M. J. Bronskill, and R. M. Henkelman, "T1, T2 relaxation and magnetization transfer in tissue at 3 T," *Magn. Reson. Med.* **54**, 507–512 (2005).
- <sup>20</sup>P. A. Bottomley, C. J. Hardy, R. E. Argersinger, and G. Allen-Moore, "A review of 1H nuclear magnetic resonance relaxation in pathology: Are T1 and T2 diagnostic?," *Med. Phys.* **14**, 1–37 (1987).
- <sup>21</sup>P. A. Bottomley, T. H. Foster, R. E. Argersinger, and L. M. Pfeifer, "A review of normal tissue hydrogen NMR relaxation times and relaxation mechanisms from 1–100 MHz: Dependence on tissue type, NMR frequency, temperature, species, excision, and age," *Med. Phys.* **11**, 425–448 (1984).
- <sup>22</sup>J. H. Zhong, J. C. Gore, and I. M. Armitage, "Relative contributions of chemical exchange and other relaxation mechanisms in protein solutions and tissues," *Magn. Reson. Med.* **11**, 295–308 (1989).
- <sup>23</sup>S. Posse, C. A. Cuenod, R. Risinger, D. Le Bihan, and R. S. Balaban, "Anomalous transverse relaxation in 1H spectroscopy in human brain at 4 Tesla," *Magn. Reson. Med.* **33**, 246–252 (1995).
- <sup>24</sup>D. N. Guilfoyle, V. V. Dyakin, J. O'Shea, G. S. Pell, and J. A. Helpen, "Quantitative measurements of proton spin-lattice (T1) and spin-spin (T2) relaxation times in the mouse brain at 7.0 T," *Magn. Reson. Med.* **49**, 576–580 (2003).
- <sup>25</sup>E. Yacoub, A. Shmuel, J. Pfeuffer, P. F. Van De Moortele, G. Adriany, P. Andersen, J. T. Vaughan, H. Merkle, K. Ugurbil, and X. Hu, "Imaging brain function in humans at 7 Tesla," *Magn. Reson. Med.* **45**, 588–594 (2001).